# Determination of Image Sources to Predict LOS Propagation in an Urban Microcell

Ho-kyung Son, Che-young Kim*
*Radio Technology Research Group, ETRI*
*161 Gajeong-dong Yuseong-gu, Daejon, 305-700, KOREA, hgson@etri.re.kr*
*Department of Electronics, Kyungpook National University in Daegu*

**Abstract**

*In this paper we describe the generalized method for the prediction of the LOS propagating characteristics in an urban Microcell using the ray tracing technique. The conventional ray tracing techniques suffer from finite number of rays and can't ensure the exact solution. But the image methods allow us to treat the infinite number of rays and thus obtain the accurate solution. Also there is the benefit of computation times and capacity. To take into account the infinite number of paths the technique of the numbering scheme of image antennas was presented by using the rectangular pulse. The proposed technique has resolved the restriction on the finite number of paths encountered in conventional ray launching methods. With application of the numbering method on the canyon model, the received power and RMS delay spread are computed and their accuracy dependence on the employed number of paths are compared and discussed at the frequencies of both 900MHz and 2.4GHz.*

## 1. INTRODUCTION

Rapid growth of mobile communication using the radio waves necessitates the research on the propagation characteristics. The mobile communication is mainly serviced in urban environments and the canyon model is used to model the urban environments. To promote the limited frequency spectrum efficiently many communication services, for instance, PCS (Personal communication System) and WLAN (Wireless Local Area Network) often has been deployed in small area as Microcell and Picocell unit. However, for satisfactory services within a confined area it needs more accurate electromagnetic analysis than those services in the large area since a quality of communication heavily influenced by nearby objects around the antennas, and scattering phenomena becomes the site-specific in nature particularly on an urban street. Thus many references on the microcell and picocell are reported [1, 2]. In this paper, the generalized method of the prediction on the LOS propagation characteristics in an urban microcell by using the ray tracing technique is proposed and emphasized on the numbering technique.

As an appropriate model to predict the propagation characteristics in microcell, the canyon model is used in this work. The model is composed of the three surface having different dielectric constants which characterize the type of buildings and ground. The ray tracing technique is used to predict the receiving power for the canyon model. This technique emphasizes on finding of the exact reflection point during the wave propagation. To determine the reflection point, the multiple-image sources generated by three different dielectric facets are used. In other words, the reflection point can be found by using the fact that the reflection waves could be regarded as those waves emanating from the associated image sources.

The canyon model is not unique one. Other authors had used this model to predict the path loss in a straight road [3-6]. But the number of paths is limited to 6~10 rays. The proposed technique extends the finite number to infinite number by introducing the image antennas and their elegant numbering scheme. For this we have employed a rectangular numbering technique on sequence of image antennas. Based on the suggested numbering technique the traditional finite number of rays could be extended to infinity and the computer algorithm is developed using this method. Input variables to the computer algorithm are the geometry of a road, medium variables of buildings and road, frequency, the position coordinate of the transmitter and receiver and the specification of antennas. As the output of simulation runs, the receiving power and RMS delay spread are computed at the frequencies of both 900MHz and 2.4GHz and some level deviations due to the number of paths are compared and analyzed.

## 2. THE DIELECTRIC MODEL

Fig. 1 shows the dielectric canyon model with road and buildings of three facets representing a lossy dielectric with the permittivity. It also depicts the 3-dimensional coordinates of the transmitter and receiver. The transmitter and receiver are positioned at $(x_t, y_t, h_t)$ and $(x_r, y_r, h_r)$ respectively. The radiation pattern of transmitting antenna determines the

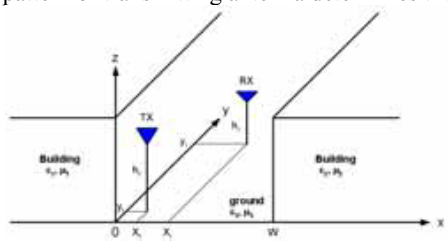

Fig. 1 The urban canyon model.

direction of propagating waves. These waves undergo multiple reflections when waves impinge on the walls of the buildings and road. The image source is used to find the exact position where the reflection occurs on walls and ground.

Let us assume that the two walls are lined infinitely along the y-axis and z-axis, and infinite ground plane along the y-axis. And also flat wall and ground are assumed. Due to the assumed flatness we can find out the precise position of image sources for walls and road, which are to be replaced by an infinite number of transmitting antennas. The total received power is a superposition of power due to the real antennas and the image antennas for ground and buildings. Therefore the total received power is found to be

$$P_R = P_T(\frac{\lambda}{4\pi})^2 \left| \sum_{n=0}^{N} (G_{nw}R_{nw}\frac{e^{-jkr_{nw}}}{r_{nw}} + G_{ng}R_{ng}\frac{e^{-jkr_{ng}}}{r_{ng}}) \right|^2 \qquad (1)$$

where $P_T$ is the transmitting power and $\lambda$ is wavelength. $G_{nw}$ and $G_{ng}$ are the image antenna gain on the ground and under the ground, respectively. $r_{nw}$ is the propagation path between image antennas on the ground and the receiver antenna. Also $r_{ng}$ is the propagation path between image antennas under the ground and the receiver antenna. The first subscript, $n$, is the number of image antennas by building walls and second subscript $w, g$ mean each image antennas lying on the ground and under the ground.

## 3. IMAGE ANTENNAS

Let us first deal with image antennas by two walls, and then deal with image antennas by a ground later. Infinite image sources by two walls are numbered as shown in Fig.2.

The real transmitting antenna TX is denoted by $T_0$, odd numbers are allocated for image antennas by two walls at $x < 0$ region and even numbers assigned at $x > w$ region.

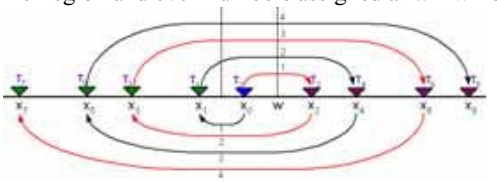

(a)

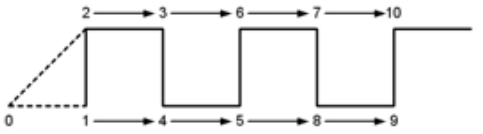


(b)

Fig. 2 The image generating process and the numbering scheme on the image antennas.
(a) The generating process and the x-coordinate of image antennas
(b) The numbering scheme of image antennas by a pulse

Fig. 2(a) shows the assigned numbers on image antennas. As shown in Fig 2(b), the rectangular pulse is complemented to designate the image antennas. The real transmitting antenna $T_0$ branches to the two image antennas, $T_1$ and $T_2$. The generated image antennas by $T_1$ have the bottom numbers on the rectangular pulse and the generating image antennas by $T_2$ have the upper numbers on that pulse. The x-axis coordinate of generated image antennas during this process are given as the second column in Table 1.

To calculate the received power using (1), we must know how many times the waves from each image antennas are reflected on wall 1 and wall 2. As shown in Fig.2 (b), the generated image antennas $T_4, T_5, T_8$ by the image antenna $T_1$ firstly undergo reflection on the wall 1, pass through other reflections and reach receiving antenna RX. On the other hand the generated image antennas $T_3, T_6, T_7$ by image antenna $T_2$ firstly undergo reflection at the wall 2, pass through the others each path and arrive at receiver antenna RX. Also the number pair of antennas which are perpendicularly located at the same position in the rectangular pulse, i.e. $(0),(1,2),(4,3),(5,6)$ … have in turn reflection times of $m_n = 0,1,2,\cdots$ and sequence $m_n$ is known at the fifth column on table 1. From this, the general formula for the total reflection times of each image antenna related to image antennas number $n$ is given by

$$m_n = \frac{(2n+1)+(-1)^{n+1}}{4} \qquad (2)$$

where $n = 0,1,2,3,\cdots$ and the reflection times of image antennas under the ground have one more by the ground than image antennas on the ground. In table 1, $b_{n1}, b_{n2}$ stand for the number of reflections on wall 1 and 2.

From table 1, the general formula for $b_{n2}$ reflection times by wall 2 can be written as

Table 1. The coordinate of image antennas and the number of reflections by each wall

| Ant. number $n$ | Coordinate of antennas $x_n$ | Reflection times by wall 1 $b_{n1}$ | Reflection times by wall 2 $b_{n2}$ | Total reflection time $m_n$ |
|---|---|---|---|---|
| 0 | $x_t$ | 0 | 0 | 0 |
| 1 | $-x_t$ | 1 | 0 | 0 |
| 2 | $-x_t + 2w$ | 0 | 1 | 1 |
| 3 | $x_t - 2w$ | 1 | 1 | 1 |
| 4 | $x_t + 2w$ | 1 | 1 | 2 |
| 5 | $-x_t - 2w$ | 2 | 1 | 2 |
| 6 | $-x_t + 4w$ | 1 | 2 | 3 |
| 7 | $x_t - 4w$ | 2 | 2 | 3 |
| 8 | $x_t + 4w$ | 2 | 2 | 4 |

$$b_{n2} = \frac{(2d_n + 1) + (-1)^{d_n + 1}}{4} \tag{3-1}$$

$$d_n = \frac{(2n-1) + (-1)^n}{4} \tag{3-2}$$

In here $n = 0,1,2,\cdots$ and the sequence $\{d_n\}$ is introduced to define the sequence $\{b_{n2}\}$. $b_{n1}$, reflection times on wall 1, is equal to $m_n - b_{n2}$.

From table 1, the coordinate of image antennas $x_n$ can be expressed using the general formula for image antenna number $n$ as

$$x_n = (-1)^{m_n} x_t + [(-1)^n m_n + \frac{1 + (-1)^{m_n + 1}}{2}]w \tag{4}$$

where $m_n$ is given by (2). $x_t$ is location of the transmitting antenna on x-coordinates and $w$ represents width of road.

The position of receiving antenna is fixed at $(x_r, y_r, h_r)$ in Fig.1. The coordinate of random n-th antenna $T_n$ or $T_{ng}$ is expressed as $(x_n, y_t, z_t)$. Therefore the distance $r_n$ between image transmitting antennas and receiving antenna is represented as following

$$r_n = \sqrt{(x_r - x_n)^2 + (y_r - y_t)^2 + (z_r - z_t)^2} \tag{5}$$

In here $x_n$ is given by equation (4). The y-coordinates of all image antennas are $y_t$, the z-coordinate is $z_t = h_t$ for image antenna on the ground and $z_t = -h_t$ for image antenna under the ground. To apply (1) to the urban model shown Fig.1, the total reflection coefficient $R_{nw}$ and $R_{ng}$ for propagation paths must be found. n-th image transmitting antenna by walls $T_n$ generates the new image source $T_{ng}$ for the ground. The transmitting wave from $T_{ng}$, real transmitting antenna TX, undergo reflection at two walls and ground, which arrive at the receiving antenna. Here the incident angle of radio wave for the ground is represented as $\theta_{ng}$. If firstly considering for image antennas on the ground, reflection coefficient for n-th radio path is given in the following

$$R_{nw} = \Gamma_{n1}^{b_{n1}} \Gamma_{n2}^{b_{n2}} \tag{6}$$

where $\Gamma_{ni}$ and $b_{ni}$ are each reflection coefficient and reflection times related to building wall $i$ (1 or 2) for n-th propagation path. $\Gamma_{ni}$ in (6) is reflection coefficient for perpendicular polarization and if the magnetic permeability of each medium is set as free space value $\mu_0$, $\Gamma_{ni}$ becomes [7]

$$\Gamma_{ni} = \frac{\cos\theta_{nw} - \sqrt{\varepsilon_{ri} - \sin^2\theta_{nw}}}{\cos\theta_{nw} + \sqrt{\varepsilon_{ri} - \sin^2\theta_{nw}}} \tag{7}$$

where $\varepsilon_{ri}$ is the relative permittivity of the i-th building , and incident angle is

$$\theta_{nw} = \sin^{-1}\left(\frac{\sqrt{(y_r - y_t)^2 + (z_r - z_t)^2}}{r_n}\right) \tag{8}$$

where $z_t = h_t$.

Each image antenna by building wall also generates the image antenna by the ground. The reflection coefficient for n-th propagation path by image antenna at $z_t = -h_t$ is represented in equation (9) and it includes the reflection by the ground.

$$R_{ng} = \Gamma_{n1}^{b_{n1}} \Gamma_{n2}^{b_{n2}} \Gamma_{nw} \tag{9}$$

where $\Gamma_{ni}$ is the same to that of equation (7) and the incident angle for buildings must be evaluated at $z_t = -h_t$. The incident wave for the ground has a parallel polarization whose direction of electric field is also parallel to the interface. Therefore $\Gamma_{ng}$ in equation (9) is reflection coefficient for the parallel polarization and shown as following [7]

$$\Gamma_{ng} = \frac{\varepsilon_{rg}\cos\theta_{ng} - \sqrt{\varepsilon_{rg} - \sin^2\theta_{ng}}}{\varepsilon_{rg}\cos\theta_{ng} + \sqrt{\varepsilon_{rg} - \sin^2\theta_{ng}}} \tag{10}$$

where $\varepsilon_{rg}$ is the relative permittivity of the ground and incident angle is given by

$$\theta_{ng} = \sin^{-1}\left(\frac{\sqrt{(x_r - x_n)^2 + (z_r - z_t)^2}}{r_n}\right) \tag{11}$$

In equation (7) and (10), each medium permittivity $\varepsilon_{ri}$ and $\varepsilon_{rg}$ are complex values.

## 4. SIMULATION RESULT

Let us show the result of mean received power calculated by equation (1). In calculation the transmitting power is set as $P_T = 10mW$. All antennas patterns are assumed to be dipole and its gain is given as [8]

$$G(\theta) = 1.64\left(\frac{\cos(\frac{\pi}{2}\cos\theta)}{\sin\theta}\right)^2 \tag{12}$$

On computation, the width of road $w = 25m$, position of transmitting antenna $x_t = 5m, y_t = 0m$, and its height $h_t = 9m$ are used. And also, the position of receiving antenna $x_r = 20m$ and its height $h_r = 1.5m$ are introduced, and $y_r$ is taken as a variable. And the permittivity of the building wall is $\varepsilon_{rw}' = 3$, $\sigma_w = 0.005 S/m$. For the road, $\varepsilon_{rg}' = 15$ and $\sigma_g = 7 S/m$ have been assigned.

Fig. 4 illustrates the receiving power at f=900MHz and f=2.4GHz, $y_r$ is varied from 0m to 500m along the y-axis. Also the receiving power is compared for propagation path number $N_T = 10, N_T = 50$. We can observe that the pattern of fading of receiving power is almost identical. The broken-dot line represents the directly received power with no obstacles in free space.

One of the important parameters together with the mean received power in digital communication is RMS (Root Mean Square) delay spread [9, 10]. When a signal is received after passing through a multiply reflected propagation media, then the signal is observed to vary with time or distance. The randomness of the variations is much severe than a single path. This phenomenon is known as fading caused by the different arriving times of each reflected waves. In order to compare the different time delay profile, the receiving pulse trains are defined by the series form of

$$p(t) = \sum_{n=1}^{N} p_n \delta(t - \tau_n) \tag{13-1}$$

$$p_n = P_T \left(\frac{\lambda}{4\pi}\right)^2 \left| G_n R_n \frac{e^{-jkr_n}}{r_n} \right|^2 \tag{13-2}$$

$$\tau_n = \frac{r_n}{c} \tag{13-3}$$

when the impulse is excited at the coordinate origin. In here $p_n$ is the amplitude of receiving power over the path n and $\tau_n$ is delayed time by such a path. $\delta(t - \tau_n)$ is a delta function or impulse function at $t = \tau_n$ and $c$ is the velocity of light. The RMS delay spread is expressed in the following

$$\Delta = \left| \frac{\sum_{n=1}^{N} \tau_n^2 p_n}{\sum_{n=1}^{N} p_n} - \left[ \frac{\sum_{n=1}^{N} \tau_n p_n}{\sum_{n=1}^{N} p_n} \right]^2 \right|^{\frac{1}{2}} \tag{14}$$

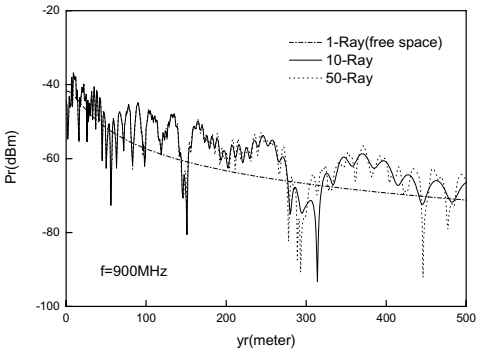


(a)

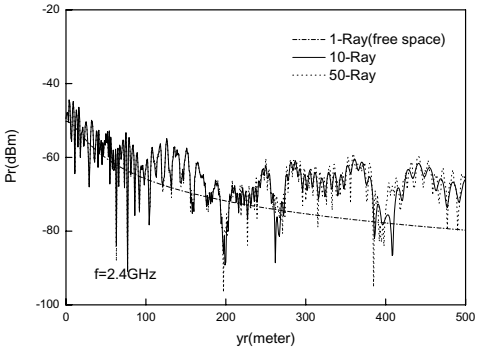


(b)

Fig. 3 The receiving power, $\varepsilon_{rw}' = 3, \sigma_w = 0.005$, $\varepsilon_{rg}' = 15, \sigma_g = 7$
(a) Frequency f=900MHz
(b) Frequency f=2.4GHz

From (14), we can see that the RMS delay spread is determined by antenna's position, gain pattern and the structure of channel. Equation (14) does not rely on the absolute power level of received signal.

Fig. 4 shows the RMS delay spread of the receiving power.

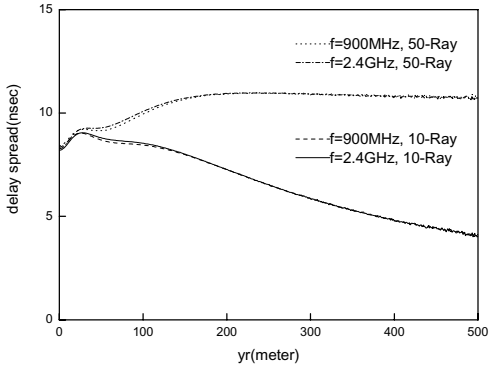


Fig.4. RMS Delay Spread
$x_r = 20m$, $\varepsilon_{rw}' = 3, \sigma_w = 0.005$, $\varepsilon_{rg}' = 15, \sigma_g = 7$

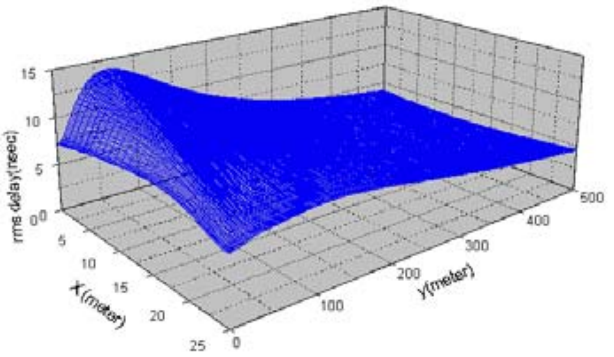


(a) The number of paths $N_T = 10$

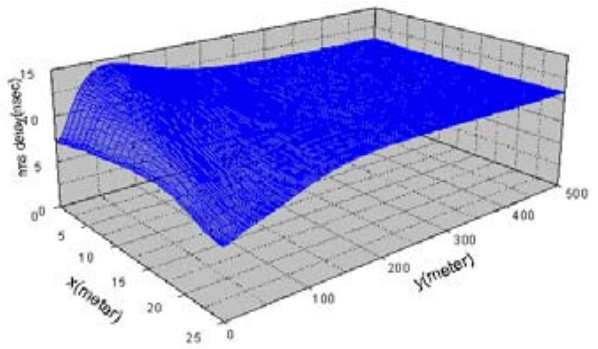


(b) The number of paths $N_T = 50$

Fig.5. RMS Delay Spread, $\varepsilon_{rw}{}' = 3, \sigma_w = 0.005$, $\varepsilon_{rg}{}' = 15, \sigma_g = 7$

In case of $N_T = 10$, it is increasing sharply near at $y_r = 30m$ and then drops at far away point. In case of $N_T = 50$, it also increases sharply at the same y-position and then shows smooth increasing at the other position, and remains the constant value after $y_r = 150m$. The delay spread heavily depends on the number of path taken. We know that more rays are required to ensure the solution convergence.

Fig. 5 shows the RMS delay spread for $N_T = 10, N_T = 50$ when the receiving point is positioned on x-y plane. The delay spread value is constant to the extent of $y_r = 200m$ even though the x-value increases along its axis.

## 5. CONCLUSIONS

This paper discussed on the characteristic of LOS propagation in an urban Microcell using the ray tracing techniques. The urban microcell is modeled as the canyon model with the three different dielectric constants. The image antennas by buildings and ground are used to find the received power in the canyon model. The proposed numbering scheme using a rectangular pulse was found to be very useful on representing these image sources, which allowed us to use infinite number of rays although conventional ray techniques suffer from finite number of rays. Allowance of treating the infinite path numbers results in finding of the exact solution on the structures to be considered. However, one could obtain this benefit as far as the flat surface is concerned. Based on the simulation result, we have observed that the receiving power needs about ten path numbers for its convergence but the delay spread requires more rays to ensure the solution convergence on the same propagation channel.

## REFERENCES


[1] S. Y. Tan and H. S. Tan, "UTD propagation model in an urban street scene for microcellular communications," *IEEE Trans. Electromagnet. Compat.,* vol. 35. pp. 423-428, Nov. 1993.

[2] Jan-Erik Berg. "A recursive method for street microcell path loss calculations," in *IEEE Int. Symp. Personal. Indoor and Mobile Radio commun.*, vol. 1, pp. 140-143, Sept. 1995.

[3] A. J. Rustako, et. al., "Radio propagation at microwave frequencies for line-of-sight microcellular mobile and personal communications." *IEEE Trans. Veh. Technol.*, vol. 40, no. 1, pp. 203-210, Feb. 1991.

[4] H. H. Xia, et. al., "Radio propagation measurements and modelling for line-of-sight microcellular system," in *Proc. Of the 42nd IEEE Veh. Technol. Conf.*, pp. 349-354, 1992

[5] N. Amitay, "Modeling and computer simulation of wave propagation in lineal line-of-sight microcells," *IEEE Trans. Veh. Technol,* vol. 41. no. 4, pp. 337-342, Nov. 1992.

[6] N. Papadakis, et. al., "Radio propagation measurements and modelling using ray tracing techniques," in *Proc. 44th IEEE Veh. Technol. Conf.*, pp. 1767-1770, June 1994

[7] J. A. Kong, *Electromagnetic Wave Theory.* Wiley, New York, pp. 110-120, 1986

[8] W. L. Stutzman and G. A. Thiele. *Antenna Theory and Design*, Wiley, New York, pp. 84-87, 1981

[9] W. C. Jakes, Jr., Ed., *Microwave Mobile Communications,* IEEE Press. pp. 45-52, 1974

[10] K. Siwiak, *Radiowave Propagation and Antennas for Personal Communications*, Artech House, pp. 158-161, 1995.